

Power-law scaling of dislocation velocity distributions: various exponents during relaxation

Péter Dusán Ispánovity,^{1,2,*} István Groma,² Géza Györgyi,² Péter Szabó,² and Wolfgang Höffelner¹

¹*Paul Scherrer Institut, CH-5232 Villigen PSI, Switzerland*

²*Department of Materials Physics, Eötvös University Budapest, H-1517 Budapest POB 32, Hungary*

Relaxation processes of dislocation systems are studied by two-dimensional dislocation dynamics simulation. Our main finding is that the power-law decay of various physical quantities is the result of the underlying scaling property of the dislocation velocity distribution. This is confirmed in three scenarios: relaxation from a random initial state, response to an added fixed dislocation of a relaxed system, or to an external shear stress below the yield stress. The exponents are different in each case, and the scaling is found to break down at a cut-off time increasing with system size. The above features are reminiscent to glassy systems, and caused by the joint effect of the long-range interaction between dislocations as well as the quenched disorder in the positions of the slip planes.

PACS numbers: 61.72.Lk, 81.40.Lm, 89.75.Da, 68.35.Rh

When crystalline materials are subjected to large enough stresses they undergo plastic (irreversible) deformation caused by the motion of dislocations. As it is well-known, these linear lattice defects interact via long-range ($1/r$ type) stress fields [1] playing a crucial role in several complex phenomena related to plasticity, such as the formation of various dislocation patterns during deformation [2] and dislocation avalanches [3]. Another characteristic of dislocation systems is the inherent randomness in the positions of slip planes, wherein individual dislocations glide easily. The interplay of long range interaction and disorder can lead to complex behavior, constituting a long time challenge for theory as well as numerical simulations.

Systems with long-range interactions, for example, self-gravitating systems [4] or non-neutral plasmas [5] have been intensively studied in the past. These systems exhibit several unique properties, like anomalous diffusion and power-law relaxation with a timescale diverging with system size [6, 7]. Whereas these systems are Hamiltonian as opposed to the strongly dissipative nature of dislocations, the complexity they exhibit indicate that anomalous behavior can be expected from dislocation systems, too. On the other hand, systems with disorder, like structural and spin glasses, show peculiar dynamic properties [8, 9]. Foremost among them is slow relaxation, attributed to a wide spectrum of decay times, as well as memory effects collectively known as aging. The fact that dislocation systems can contain quenched disorder in the position of easy glide planes raises the analogy with spin glasses. Glassy dynamical behavior has indeed been observed in simulations [10] and experimentally [11] for dislocation systems, but the phenomenon is still lacking a systematic study. In this Letter we focus on the properties of relaxation to equilibrium below the yield stress in a two-dimensional (2D) dislocation system with one slip axis. We find that this system, which is subject of growing interest [12–14], exhibits power decay with various exponents due to the underlying scaling of

the dislocation velocity distribution, breaking down at a cut-off time increasing with system size.

Slow relaxation has been already observed in 2D dislocation systems. It was found [15] that under constant external stress, i.e., creep condition, a dislocation system with single slip exhibits the well-known Andrade-type creep law [16], with the plastic strain rate $\dot{\gamma}_{\text{pl}}$ decreasing in time t as $\dot{\gamma}_{\text{pl}}(t) \sim t^{-2/3}$ until a cut-off time t_1 . It was also shown that t_1 tends to infinity as some critical stress is approached from below, providing a straightforward analogy between the yielding transition and conventional phase transitions [15, 17]. In addition, it was also reported earlier that single slip random 2D dislocation systems at zero external stress relax to an equilibrium state slowly, with a relaxation time increasing with the system size [18, 19]. Such slow relaxation processes of dislocated crystals have been also observed experimentally [16, 20].

The aim of this Letter is to show that all the power-law relaxation properties reported earlier [15, 18, 19] are the result of the scaling of the velocity distribution of the dislocations. The system considered is the simplest representation of a dislocated crystal, consisting of parallel straight edge dislocations with parallel slip planes. Thus the problem is simplified to 2D. By denoting the position of the i th dislocation by $\mathbf{r}_i = (x_i, y_i)$, its Burgers vector by $\mathbf{b}_i = s_i(b, 0)$ ($s_i = \pm 1$ is the sign of the “charge”), the equation of motion of a single dislocation can be written in the form

$$\dot{x}_i = s_i \left[\sum_{j=1; j \neq i}^N s_j \tau_{\text{ind}}(\mathbf{r}_i - \mathbf{r}_j) + \tau_{\text{ext}}(\mathbf{r}_i) \right]; \quad \dot{y}_i = 0. \quad (1)$$

Here τ_{ind} is the shear stress field generated by an individual dislocation:

$$\tau_{\text{ind}}(\mathbf{r}) = \frac{x(x^2 - y^2)}{(x^2 + y^2)^2} = \frac{\cos(\varphi) \cos(2\varphi)}{r}, \quad (2)$$

τ_{ext} denotes the external shear stress, and N is the to-

tal number of the constituent dislocations. It is important to note that the different physical parameters are absorbed in the length-, time-, and stress-scales, as we measure them in $\rho^{-0.5}$, $(\rho M G b^2)^{-1}$, and $G b \rho^{0.5}$ units, respectively, where ρ is the dislocation density, M is the dislocation mobility, and G is an elastic constant [19]. So, in the rest of this Letter, only these dimensionless units are used.

Let us highlight the most important physical features of this conceptually simple model. Firstly, the pair interaction is of long-range character, since it decays with $1/r$, moreover, it exhibits a complicated angular dependence with zero average. Secondly, the equation of motion (1) is first order, which is due to the commonly assumed overdamped nature of dislocation motion, thus the system is strongly dissipative, i.e., non-Hamiltonian. Thirdly, the motion is constrained, since dislocations can only move parallel to the x axis. This has the important consequence that if the initial y coordinates are chosen randomly then this will represent quenched disorder. As a result, the system never completely forgets its initial state, that is, it does not collapse into a global energy minimum, rather gets trapped into a local energy minimum. Thus, the ground state of the system is frustrated leading to a glassy-like dynamics [10].

In the first part of this Letter the relaxation of random dislocation systems is studied. In this scenario an equal number of positive ($s_i = 1$) and negative ($s_i = -1$) sign dislocations are placed randomly in a square-shaped area. Then, with periodic boundary conditions, the equations of motion (1) are solved numerically [19] until no considerable dislocation movement is observed. The simulations were repeated with different initial configurations 13000, 300, and 118 times for the system sizes of $N = 128, 512, \text{ and } 2048$, respectively. During the relaxation of the system, the time dependent probability distribution of the dislocation velocities $P(v, t)$ was determined numerically. (Since there is no external stress, for symmetry reasons, the velocity distribution of positive and negative dislocations are equal and symmetric.) According to Fig. 1(a) a remarkable feature of the velocity distribution is that it decays to zero as v^{-3} (for a theoretical explanation see [21]). In addition, $P(v, t)$ tends to a Dirac-delta function (corresponding to the equilibrium state) and between an initial t_0 and a cut-off time t_1 this is described with the scaling law

$$P(v, t) = t^\alpha f(t^\alpha v). \quad (3)$$

The exponent α was found to be $\alpha = 0.87(2)$ and the scaling function f can be well approximated by the form $f(x) \approx A/(Bx^3 + 1)$. Note, that the curves plotted are always results of averaging over the statistical ensemble.

To investigate this scaling behavior in more detail, the m th moment $\langle |v(t)|^m \rangle$ of the absolute velocity was also

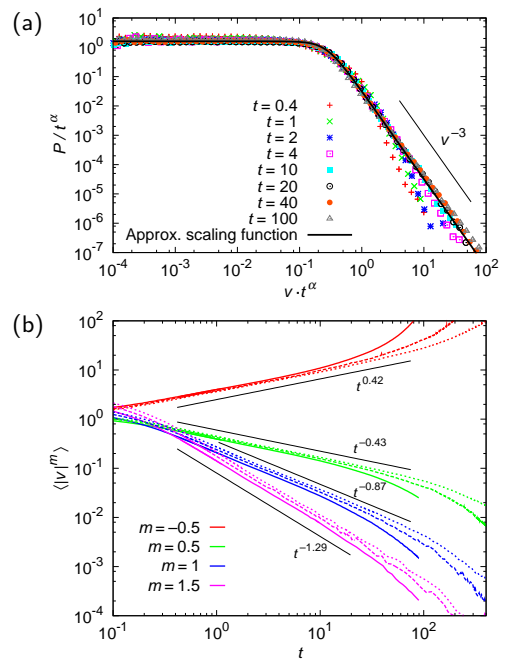


FIG. 1: (color online) Dynamics during relaxation from a random configuration. (a) The scaled velocity distributions of dislocations P_v given by Eq. (3) with $\alpha = 0.87$ at system size $N = 2048$, and the approximated fitted scaling function (see text). (b) The moments $\langle |v(t)|^m \rangle$ for different exponents m (identified by colors) and dislocation numbers N . The solid, dashed, and dotted lines correspond to $N = 128, 512, \text{ and } 2048$, respectively.

determined for different m values. According to Eq. (3)

$$\langle |v(t)|^m \rangle = \int |v|^m P(v, t) dv = C_m t^{-m\alpha}, \quad (4)$$

where C_m is a constant. (Because of the asymptotic properties of the scaling function f , the integral is finite only for $-1 < m < 2$.) Figure 1(b) shows the measured $\langle |v(t)|^m \rangle$ curves for $m = -0.5, 0.5, 1, 1.5$ and different system sizes. The fitted exponents are in agreement with Eq. (4). (With the same simulation setup scaling regime and the value of α has been already reported in [18, 19], but only for the $m = 1$ case.)

As seen in Fig. 1(b) the scaling region is bounded from both sides. It starts at a fixed $t_0 \approx 0.5$ and lasts till a cut-off time t_1 increasing with increasing linear system size $L = \sqrt{N}$. This is in perfect accordance to what is usually found in systems with long-range interactions. The actual t_1 versus L relation is analyzed below.

To understand the role of the specific mobility law (1) in the observed phenomenon, we repeated the simulations with an artificial mobility law, where the magnitude of the acting force is proportional to the square of the local stress. According to Fig. 2 the scaling still holds, but with a slightly different exponent α and scaling function.

In the second simulation scenario, an extra dislocation with fixed position is introduced to an already relaxed

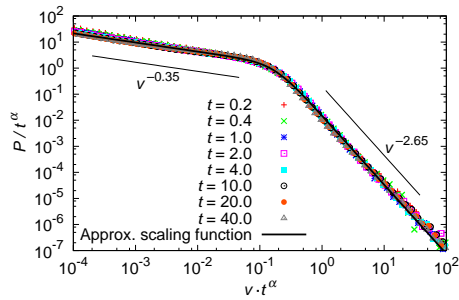


FIG. 2: (color online) Scaling of the velocity distribution as in Eq. (3) during the relaxation from a random initial state using the quadratic mobility law with $\alpha = 0.9$ at $N = 2048$. The scaling function is approximated by $f(x) \approx A/(Bx^{2.65} + x^{0.35})$.

configuration. This can be considered as the prototype of an external perturbation. (The equilibrium dislocation configuration generated by the extra dislocation, the analogue of Debye-screening, was analyzed in [22, 23].) Due to the extra force field, the system evolves to a new equilibrium state. As Fig. 3 shows $P(v, t)$ obeys again the

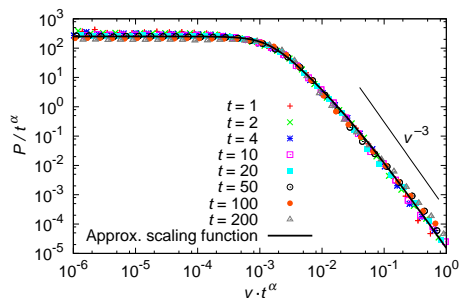


FIG. 3: (color online) Scaling of the velocity distribution after adding an extra fixed dislocation to a relaxed system with $\alpha = 0.44$ at $N = 2048$. The corresponding scaling function is $f(x) \approx A/(Bx^3 + Cx^2 + 1)$.

same scaling law given by Eq. (3), now with $\alpha = 0.44(2)$. Consistently, the evolution of different velocity moments obey Eq. (4), and thus confirms scaling.

In the third scenario an external constant shear stress τ_{ext} is turned on to the relaxed system (creep experiment first studied by Miguel et al. [13, 15]). If τ_{ext} is smaller than a certain yield stress, the induced mean plastic strain rate $\dot{\gamma}_{\text{pl}}(t)$ decreases to zero. Figure 4(a) shows the evolution of $\dot{\gamma}_{\text{pl}}$ at different external stresses τ_{ext} and system sizes N . As seen $\dot{\gamma}_{\text{pl}}$ also has a scaling regime with exponent slightly decreasing with increasing τ_{ext} . Like for the relaxation problem analyzed above, the upper cut-off t_1 is increasing with the system size but it is practically independent from τ_{ext} . This is a somewhat different conclusion from what was drawn by Miguel et al. [13, 15]. They found that at a critical stress level $\dot{\gamma}_{\text{pl}}(t)$ becomes pure power-law without a cut-off. According to our investigations the cut-off t_1 observed is in fact a finite

size effect.

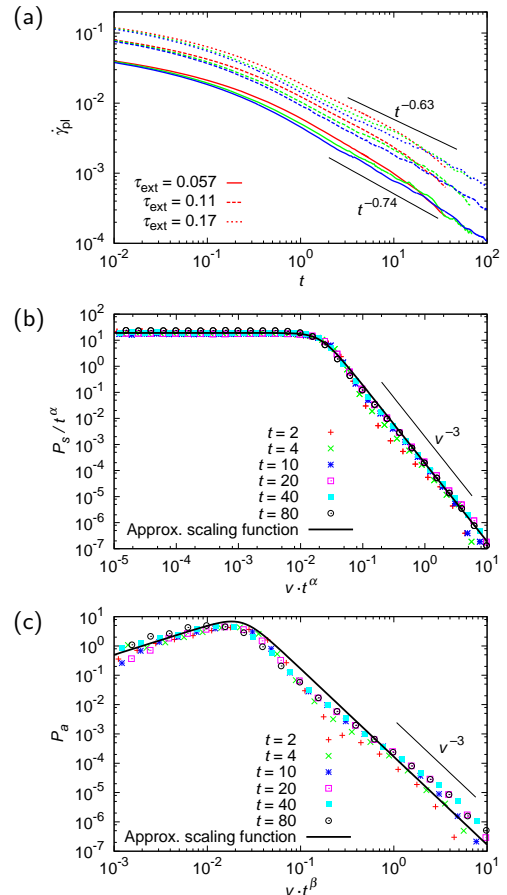


FIG. 4: (color online) Relaxation due to a constant external shear stress τ_{ext} below the yield stress. (a) The mean plastic strain rate $\dot{\gamma}_{\text{pl}}$ versus time t curves for different τ_{ext} and system sizes N . The curves with increasing cut-off (red, green, and blue) correspond to $N = 128, 512$, and 2048 , respectively. (b) The symmetric part of the velocity distribution P_s at different times scaled with Eq. (6) with $\alpha = 0.34$ at $N = 2048$ and $\tau_{\text{ext}} = 0.11$. The approximate scaling function is $f(x) \approx A/(Bx^3 + 1)$. (c) The antisymmetric part of the velocity distribution P_a at different times scaled with Eq. (6) with $\beta = 0.34$ at $N = 2048$ and $\tau_{\text{ext}} = 0.11$. The approximate scaling function is $g(x) \approx C/(Dx^3 + x^{-1})$.

To see if a similar underlying scaling property is present during the creep experiments as before, again, the velocity distribution P was analyzed. In this case, however, the distribution is not symmetric and it is different for the positive and negative sign dislocations (denoted by P^+ and P^- , respectively). For symmetry reasons $P^+(v, t) = P^-(-v, t)$, so it is enough to investigate P^+ , denoted by P . The distribution can be separated into a symmetric and an antisymmetric part: $P = P_s + P_a$. With this in the definition of the velocity moments [Eq. (4)] P has to be replaced by P_s , while $\dot{\gamma}_{\text{pl}}$

can be given as

$$\dot{\gamma}_{\text{pl}}(t) = \left\langle \sum_{i=1}^N s_i v_i \right\rangle = \int v P_a(v, t) dv. \quad (5)$$

Figure 4(b) and (c) show the scaling of P_s and P_a , respectively, for $\tau_{\text{ext}} = 0.11$ with

$$P_s(v, t) = t^\alpha f(t^\alpha v) \quad \text{and} \quad P_a(v, t) = g(t^\beta v), \quad (6)$$

at $\alpha = 0.34(2)$ and $\beta = 0.34(3)$, numerically indistinguishable. Note, that no power prefactor was found in the scaling form of P_a above. From Eqs. (5,6)

$$\dot{\gamma}_{\text{pl}}(t) = C t^{-2\beta}, \quad (7)$$

with an appropriate C constant. This is in complete agreement with the time evolution of $\dot{\gamma}_{\text{pl}}$ plotted in Fig. 4(a). For different τ_{ext} values, the same scaling is found with slightly different exponents. We mention that the plastic strain $\gamma_{\text{pl}}(t)$ has the exponent $1 - 2\beta$, this varies in the range $0.26 - 0.37$, and is in accordance with the well-known power $1/3$ of the primary Andrade creep [15, 16].

To summarize the above findings, the scaling formulas Eq. (6) seem to be generally valid. The exponents vary, however, a feature we attribute to the difference in the initial and boundary conditions for the same mobility law. Thus, the exponent is not an inherent characteristic of the dislocation system.

The last issue to be elucidated is the system size dependence of the cut-off time t_1 . In order to determine t_1 , $t^\alpha \langle |v(t)| \rangle$ is plotted with a semilogarithmic scale in Fig. 5 for the first simulation scenario. As seen, the curves obtained can be well fitted by straight lines, so the time evolution of $\langle |v| \rangle$ can be described with the form

$$\langle |v(t)| \rangle = C t^{-\alpha} \exp(-t/t_1). \quad (8)$$

Thus the cut-off time t_1 is a simple relaxation time. In

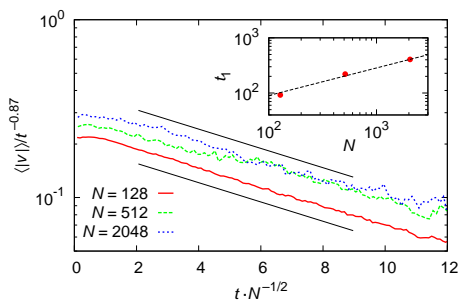


FIG. 5: (color online) Rescaled mean absolute velocity $t^\alpha \langle |v(t)| \rangle$ as a function of scaled time t/\sqrt{N} at different system sizes. Straight line on the semilog plot shows the exponential component, defining a relaxation time t_1 for each size. Inset shows the obtained t_1 values and the $t_1 \sim \sqrt{N}$ fit (dashed line).

addition, in Fig. 5 the time is rescaled with $L = \sqrt{N}$ and with this the curves corresponding to different system sizes are parallel, indicating that t_1 is proportional to the system size L . Similar behavior is found for the different order velocity moments introduced above and for the plastic strain rate $\dot{\gamma}_{\text{pl}}$. These results indicate that the relaxation of $\langle |v(t)| \rangle$ can be described with the rate equation

$$\frac{d\langle |v(t)| \rangle}{dt} = - \left(\frac{\alpha}{t} + \frac{1}{t_1} \right) \langle |v(t)| \rangle, \quad (9)$$

where $t_1 \propto L$. This can be interpreted as follows: at large enough time ($t \gg t_1$) during the relaxation of a dislocation system with finite size it always gets close to its energy minimum and enters into an exponential relaxation regime. With increasing system size, however, due to the long-range dislocation-dislocation interactions and the quenched disorder caused by the slip planes introduced randomly, the energy landscape becomes more and more complex resulting in a longer time to reach the exponential relaxation regime. In the thermodynamic limit the relaxation becomes scale free. This is in agreement with the recent results of Laurson et al. [14], who found that the dynamics slow down dramatically as the yield stress is approached from above. We would also like to highlight that although the time exponent α varies with conditions of the relaxation, the size-dependence of the cut-off time t_1 is in all cases close to linear.

In summary, slow relaxation was observed in three different simulation set-ups, with a relaxation timescale diverging with linear system size. The observed scaling property means that on the level of the velocity distribution, a natural measure of the dynamics, the distance from the equilibrium state can be expressed by a single variable decreasing as a power-law with various scaling exponents. This is remarkable, since the system itself is rather complicated, with anisotropic interactions and strongly constrained motion, as emphasized in the introduction. It is also important to stress that according to the presented results the observed scaling and slow relaxation is the consequence of the long-range nature of the interactions.

The authors thank P. Derlet for stimulating discussions. Financial supports of the Hungarian Scientific Research Fund (OTKA) under Contract No. K 67778 and The European Union and the European Social Fund under the Grant Agreement No. TÁMOP-4.2.1/B-09/1/KMR-2010-0003 are gratefully acknowledged.

* Electronic address: ispanovity@metal.elte.hu;
URL: <http://dislocation.elte.hu>

[1] J. P. Hirth and J. Lothe, *Theory of Dislocations* (John Wiley & Sons, New York, 1982), 2nd ed.

- [2] M. Zaiser and A. Seeger, *Dislocations in Solids* (North-Holland, Amsterdam, 2002), vol. 11, chap. Long-range internal stresses, dislocation patterning and work-hardening in crystal plasticity, pp. 1–100.
- [3] F. F. Csikor, C. Motz, D. Weygand, M. Zaiser, and S. Zapperi, *Science* **318**, 251 (2007).
- [4] T. Padmanabhan, *Phys. Rep.* **188**, 285 (1990).
- [5] D. R. Nicholson, *Introduction to Plasma Theory* (Wiley, New York, 1983).
- [6] A. Campa, T. Dauxois, and S. Ruffo, *Phys. Rep.* **480**, 57 (2009).
- [7] F. Bouchet, S. Gupta, and D. Mukamel, *Physica A* **389**, 4389 (2010).
- [8] V. Ilyin, I. Procaccia, I. Regev, and N. Schupper, *Phys. Rev. E* **77**, 061509 (2008).
- [9] C. Chamon and L. F. Cugliandolo, *Prog. Probab.* **62**, 225 (2009).
- [10] B. Bakó, I. Groma, G. Györgyi, and G. T. Zimányi, *Phys. Rev. Lett.* **98**, 075701 (2007).
- [11] S. J. Gerbode, U. Agarwal, D. C. Ong, C. M. Liddell, F. Escobedo, and I. Cohen, *Phys. Rev. Lett.* **105**, 078301 (2010).
- [12] G. Tsekenis, N. Goldenfeld, and K. A. Dahmen, *Phys. Rev. Lett.* (2011), (accepted for publication).
- [13] J. Rosti, J. Koivisto, L. Laurson, and M. J. Alava, *Phys. Rev. Lett.* **105**, 100601 (2010).
- [14] L. Laurson, M.-C. Miguel, and M. J. Alava, *Phys. Rev. Lett.* **105**, 015501 (2010).
- [15] M.-C. Miguel, A. Vespignani, M. Zaiser, and S. Zapperi, *Phys. Rev. Lett.* **89**, 165501 (2002).
- [16] F. Nabarro, *Acta Mater.* **54**, 263 (2006).
- [17] M. Zaiser, *Adv. Phys.* **55**, 185 (2006).
- [18] F. F. Csikor, B. Kocsis, B. Bakó, and I. Groma, *Mater. Sci. Eng. A* **400/401**, 214 (2005).
- [19] F. F. Csikor, M. Zaiser, P. D. Ispánovity, and I. Groma, *J. Stat. Mech.* (2009), P03036.
- [20] F. Louchet and P. Duval, *Int. J. Mater. Res.* **100**, 10 (2009).
- [21] P. D. Ispánovity, I. Groma, G. Györgyi, F. F. Csikor, and D. Weygand, *Phys. Rev. Lett.* **105**, 085503 (2010).
- [22] I. Groma, G. Györgyi, and B. Kocsis, *Phys. Rev. Lett.* **96**, 165503 (2006).
- [23] P. D. Ispánovity, I. Groma, and G. Györgyi, *Phys. Rev. B* **78**, 024119 (2008).